Cell, Volume *135*

Supplemental Data

Hypothalamic IKKβ/NF-κB and ER Stress Link Overnutrition to Energy Imbalance and Obesity

Xiaoqing Zhang, Guo Zhang, Hai Zhang, Michael Karin, Hua Bai, and Dongsheng Cai

Supplemental Experimental Procedures

Chemicals, Antibodies, Plasmids and Mutations. Recombinant TNF-α was purchased from Calbiochem. Recombinant LIF was purchased from Millipore. Primary monoclonal anti-pY was purchased from Upstate Biotechnology; rabbit antibodies included anti-IRS-2, anti-IRβ, anti-p85, anti-pErk1/2, anti-Erk1/2, anti-SOCS3, anti-GFP (Santa Cruz) and anti-Cre (Covance) antibodies. Super-shift antibodies included anti-p50 (Santa Cruz) and anti-p65 (provided by S. Miyamoto) antibodies. Plasmid pcDNA3.1 with $IKK\beta^{CA}$ or $I\kappa B\alpha^{SR}$ was described previously (Cai et al., 2004; Cai et al., 2005). A *firefly* luciferase plasmid with murine SOCS3 promoter (SOCS3-pGL3) was provided by Dr. R. Bruick. Deletion of putative NF-κB consensus in SOCS3-pGL3 was performed using a mutagenesis kit (Invitrogen).

Cell Culture and Luciferase Assay. GT1-7 cells (provided by Dr. P. Mellon), HEK 293-lepR (provided by Dr. L. Rui), HEK 293, HEK 293T, and C2C12 cells (ATCC) were maintained in DMEM with 5-10% FBS, glutamine, antibiotics, and in 5-10% CO_2 at 37°C. Transfection of cultured cells with luciferase plasmids and expression plasmids was performed through Lipofectamine (Invitrogen). Co-transfection of pRL-TK (Promega) was used to internally control

firefly activity. Empty plasmids pGL3 and pcDNA3.1 were used as negative controls.

Biochemical Assays. Tissue glucose content in the hypothalamus was measured using Amplex® Red Glucose/Glucose Oxidase Assay Kit (Invitrogen). For super-shift analysis of NF-κB gel shift, tissue lysate was incubated with anti-p65 or anti-p50 antibody, subjected to reaction with the NF-κB probe, then gel separation, and exposure to X-ray film.

Supplementary Table

Table 1. Expression profiles of proinflammatory and signaling genes in the hypothalamus of mice with HFD- or hyperphagia-induced obesity.

Genes	HFD/Chow (C57BL/6)			$Ob^{+/+}$/WT (Chow)		
	Fold	SEM	p	Fold	SEM	p
IKKβ	1.43	0.06	0.01*	1.76	0.14	0.00**
IκBα	2.06	0.22	0.02*	19.97	6.82	0.03*
TNFα	1.42	0.46	0.75	0.68	0.21	0.40
IL1β	0.90	0.25	0.69	243.00	71.23	0.02*
IL10	0.79	0.20	0.67	0.53	0.19	0.43
IL15	1.11	0.26	0.77	0.43	0.29	0.23
IL1βR1	0.89	0.13	0.80	2.89	0.88	0.08
TNFαR	0.96	0.11	0.76	0.80	0.08	0.18
TLR2	1.11	0.13	0.59	1.47	0.29	0.23
gp130	1.28	0.19	0.20	0.59	0.26	0.18
SOCS3	2.27	0.13	0.00**	1.99	0.33	0.03*

Quantitative RT-PCR data represent fold increase over dietary control or unaffected littermates. HFD, high fat diet. Statistical analyses: mean±SEM; *$p<0.05$, **$p<0.01$, n=4 mice/group.

Supplementary Figures

Figure S1.

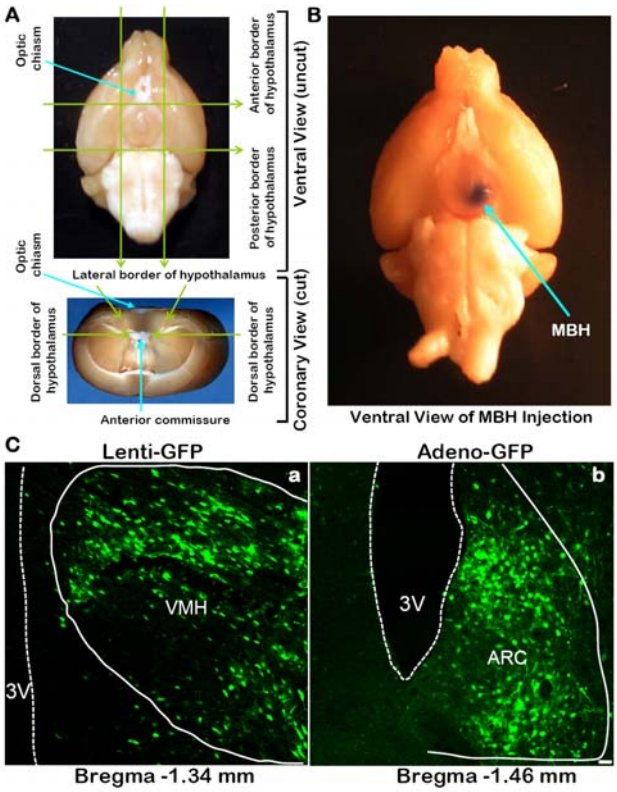

Dissection and site-specific injections of the hypothalamus. **A**. Dissection of the hypothalamus was presented by demonstrating the boundaries between the hypothalamus and the neighboring brain tissues both from a ventral (uncut) view (top) and a coronary (cut) review (bottom). **B.** Gross view of the isolated hypothalamus in the mice that received a unilateral injection of a blue dye into the MBH. **C.** Virus-mediated lateral delivery of GFP in the MBH. GFP expression was induced specifically in the MBH of C57BL/6 mice through an intra-MBH injection of either a GFP-expressing lentivirus (Lenti-GFP) (**a**) or a GFP-expressing adenovirus (Adeno-GFP) (**b**). The brain sections across the VMH at 1.34 mm posterior to Bregma (**a**) and across the ARC at

1.46 mm posterior to Bregma (**b**) were prepared and directly examined for GFP fluorescence without immunostaining. Broken lines outline 3V, and solid lines outline the VMH and ARC. Bar = 50 μm.

Figure S2.

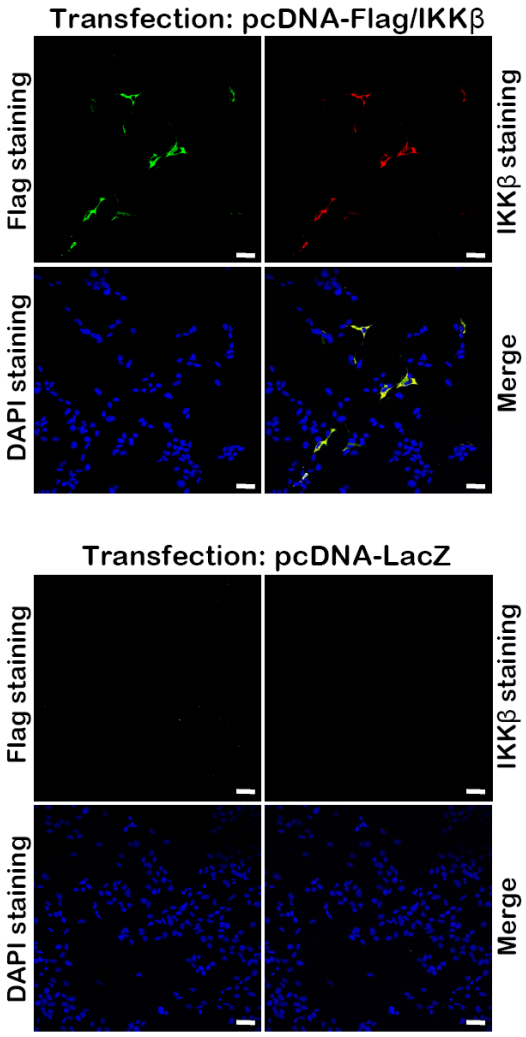

Immunostaining for plasmid-induced expression of IKKβ in GT1-7 cells. GT1-7 cells were transfected with a pcDNA plasmid containing Flag tag-conjugated IKKβ (pcDNA-Flag/IKKβ) or

an irrelevant control LacZ (pcDNA-LacZ). Following 36 hours post-transfection, the cells were fixed, and the conjugated protein was immunostained with anti-Flag and anti-IKKβ antibodies, and examined for the co-localization of Flag (green) and IKKβ (red) in the cells. The nuclear staining of DAPI revealed all the cells on the slide. Bar = 50 μm.

Figure S3.

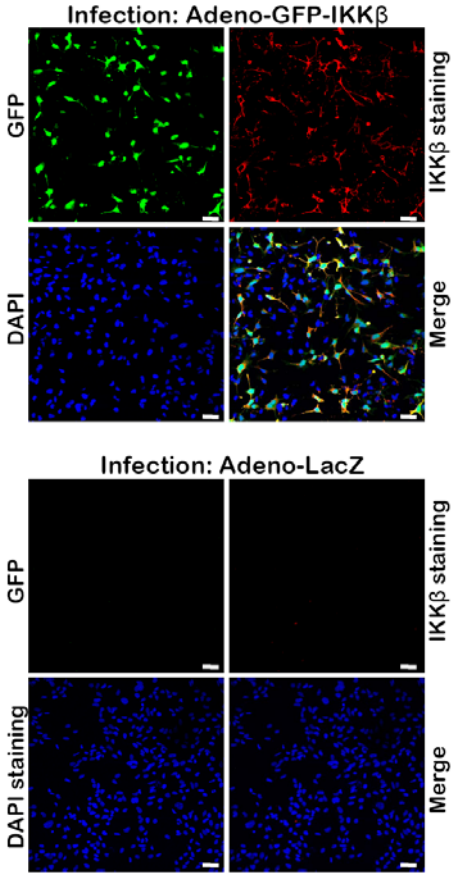

Immunostaining for viral-induced expression of IKKβ in GT1-7 cells. GT1-7 cells were infected with an adenovirus that co-expresses two individual proteins, IKKβ and GFP (Adeno-GFP-IKKβ), or with an adenovirus that expresses an irrelevant control LacZ (Adeno-LacZ). Following 36 hours post-viral infection, the cells were fixed, and the expression of IKKβ was

immunostained with anti-IKKβ antibody (red), while the GFP expression was directly detected by the green fluorescence of GFP (green). The distribution of IKKβ and GFP in the same cells was revealed by the merged images. The nuclear staining of DAPI revealed all the cells on the slide. Bar = 50 μm.

Figure S4.

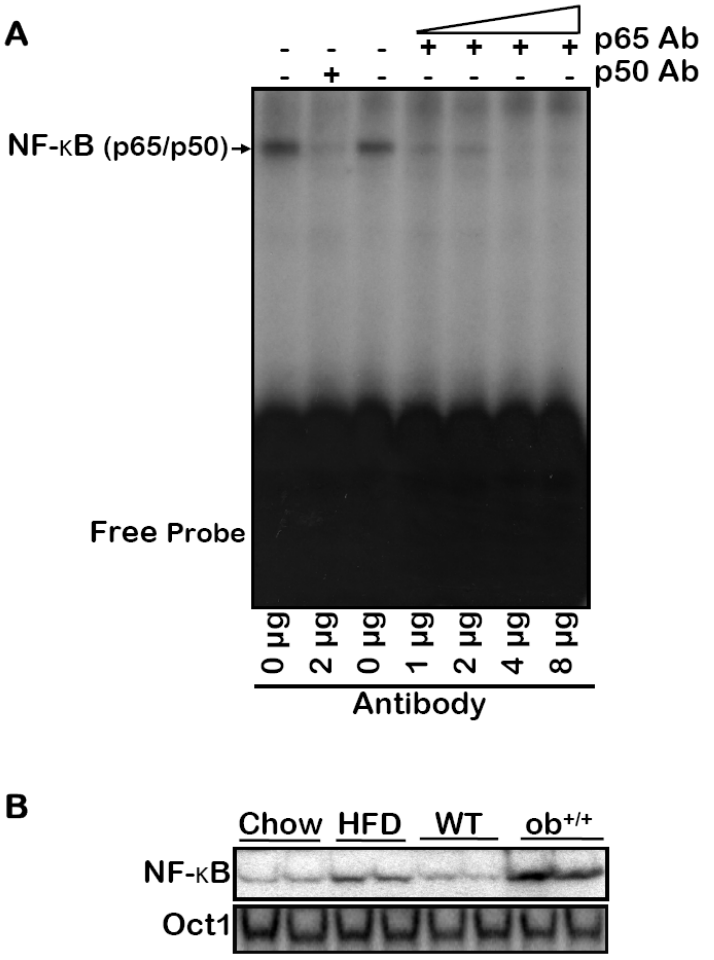

The NF-κB complex in the hypothalamus and the activity changes in the hypothalamus of obesity models. **A.** DNA-binding results of hypothalamic NF-κB were verified by a super-shift

assay using antibodies (Ab) that recognize the two components of the classical NF-κB complex, p65 and p50, at the indicated doses. **B.** The DNA binding activity of NF-κB oligo and an irrelevant control (Oct1) was measured using EMSA in the hypothalamus from HFD- *vs.* chow-fed C57BL/6 mice and chow-fed ob$^{+/+}$ mice *vs.* littermate wildtype (WT).

Figure S5.

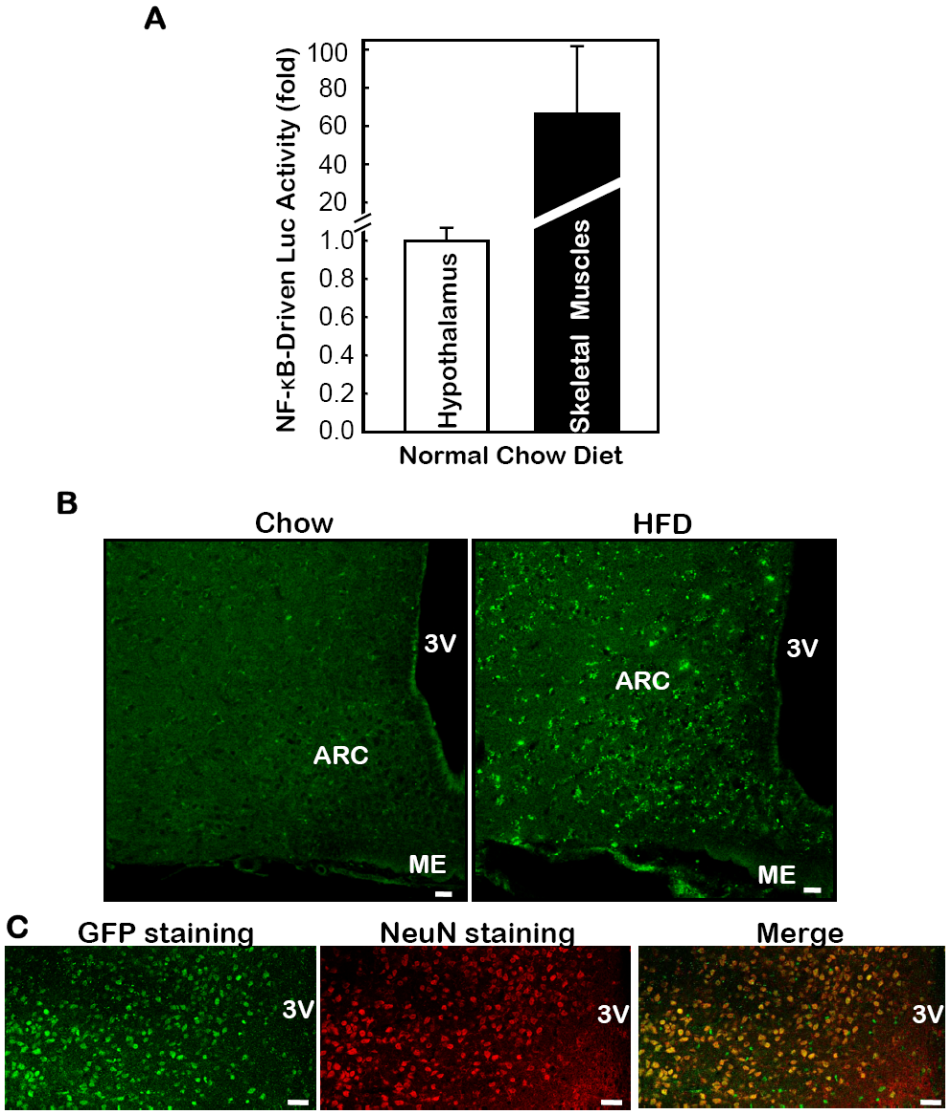

NF-κB activity in the hypothalamus of chow- and HFD-fed reporter mice. **A.** The hypothalamus and skeletal muscles (gastrocnemius) were isolated from normal chow-fed adult NGL mice that possessed normal body weights and metabolic profiles. NF-κB-driven luciferase activity in these tissues was measured and normalized by the protein contents. (n = 4 per group; *$p<10^{-4}$). **B.** The brain sections across the MBH of the NF-κB reporter mice fed normal chow *vs.* HFD were directly examined for eGFP (without staining) to report the spatial distribution of NF-κB activity. Bar = 50 μm. **C.** The brain sections across the MBH of HFD-fed reporter mice were co-immunostained using anti-GFP (green) and anti-NeuN (red) antibodies. The distribution of GFP in the MBH neurons is shown in the merged (yellow) color. Bar = 50 μm. Error bars reflect mean ± SEM.

Figure S6.

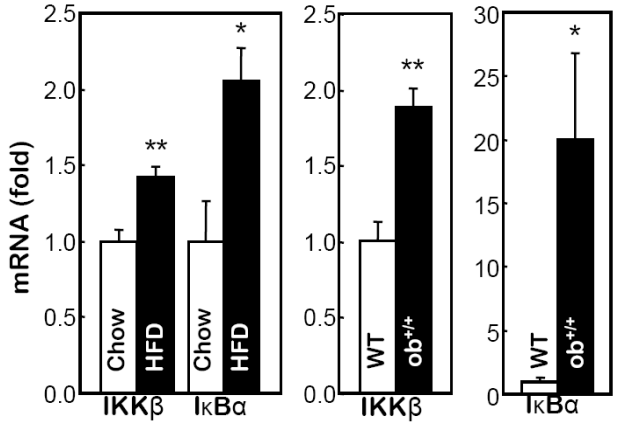

Relative mRNA levels were determined by quantitative RT-PCR in the hypothalamus of HFD-*vs.* normal chow-fed C57BL/6 mice or normal chow-fed $ob^{+/+}$ mice *vs.* littermate wildtype (WT). (n = 4-5 per group, *p<0.05, **p<0.01). Error bars reflect mean ± SEM.

Figure S7.

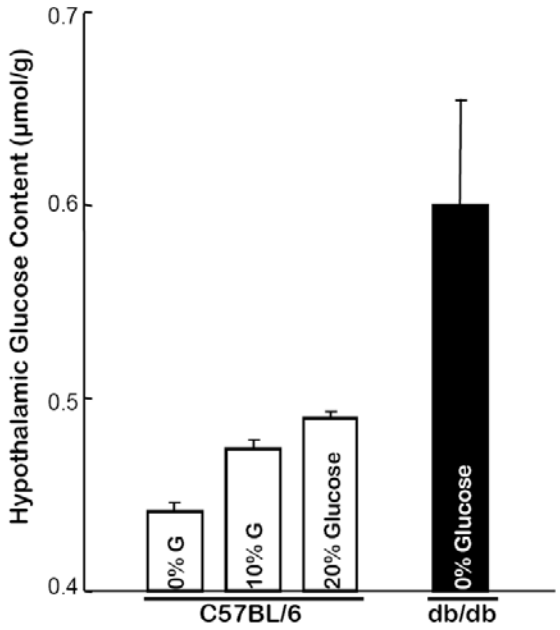

Glucose content in the hypothalamus of the mouse models. Chow-fed C57BL/6 mice received 6-hour intra-third ventricle infusions of glucose (G) at the indicated doses. The tissue lysate of the hypothalamus was measured for glucose content. The glucose content in the hypothalamus of db/db mice was also measured for the comparisons. The total protein levels of the hypothalamic lysate were used for normalization. (n = 3-4 per group). Error bars reflect mean ± SEM.

Figure S8.

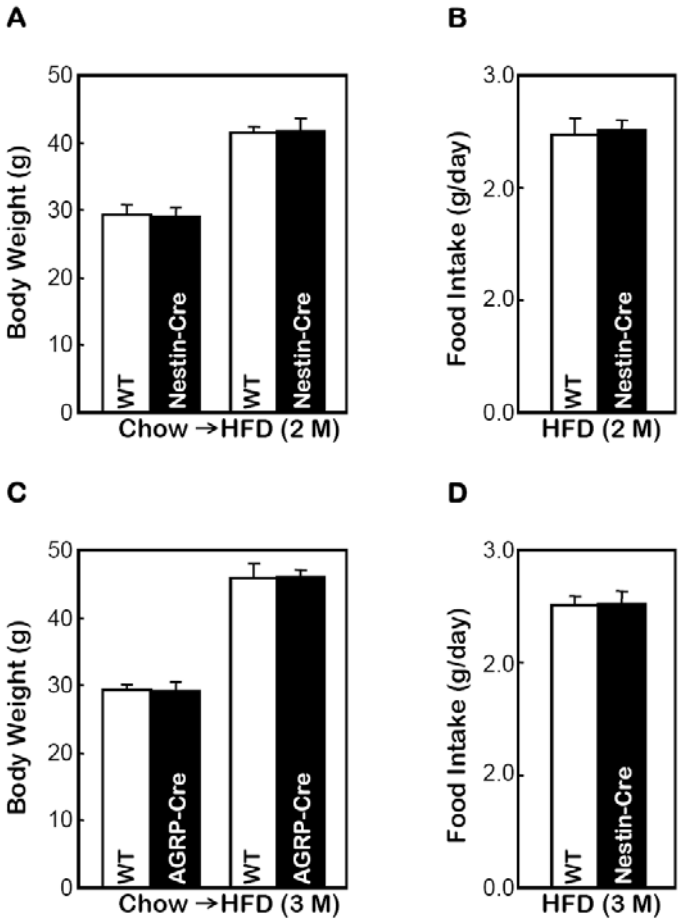

Body weight and food intake in HFD- *vs.* chow-fed Nestin-Cre and AGRP-Cre mice. Nestin-Cre mice (**A & B**), AGRP-Cre mice (**C & D**), and their littermate wildtype controls (WT) (**A-D**) were fed a normal chow following weaning and switched to a HFD for 2 or 3 months (M). Body weight and food intake of these mice were recorded. The data present the body weight (**A & C**) and food intake (**B & D**) of these mice that were measured immediately before and following the completion of HFD feeding. (n = 4-6 per group). Error bars reflect mean ± SEM.

Figure S9.

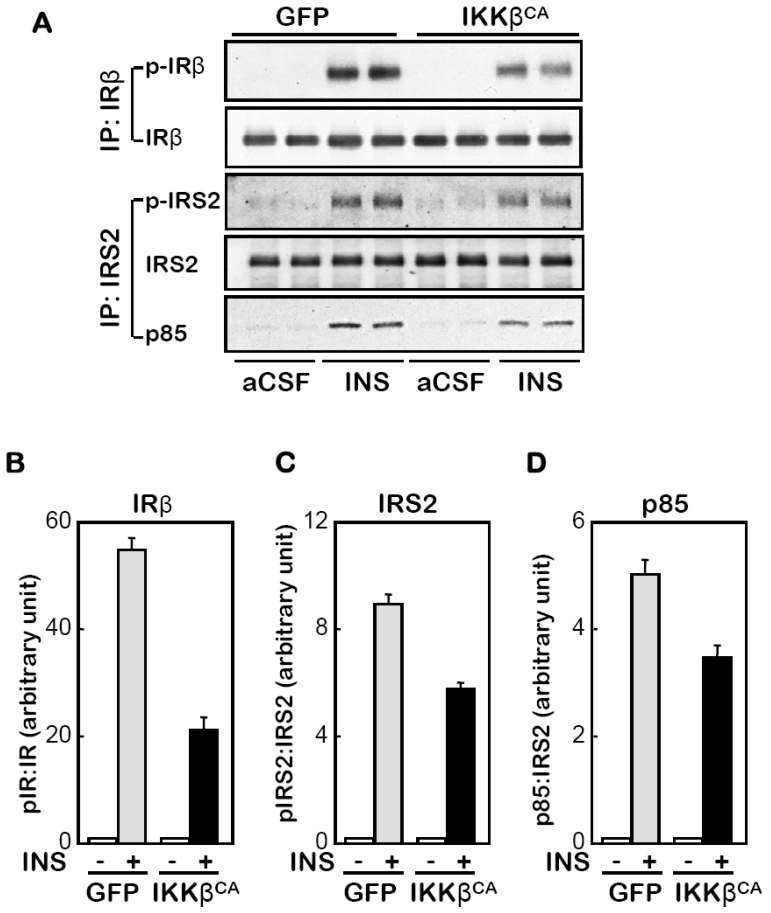

IKKβ/NF-κB activation in the MBH de-sensitizes hypothalamic insulin signaling. **A.** An adenovirus was injected into adult C57BL/6 mice to deliver either $IKK\beta^{CA}$ to both sides of the MBH of one group of mice or GFP to both sides of the MBH of another group of mice. Recovered mice were fasted for 24 hours and received third-ventricle injections of insulin (INS) and the empty vehicle (aCSF). Proteins in the dissected hypothalamus were immunoprecipitated (IP) and/or immunoblotted (IB) with the indicated antibodies. **B-D.** Phosphorylation levels of IRβ (**B**), IRS2 (**C**) and the binding of p85 to IRS2 (**D**) were quantitated and normalized

according to the protein levels of IR and IRS2, as indicated. -: aCSF. +: insulin (INS). Error bars reflect mean ± SEM.

Figure S10.

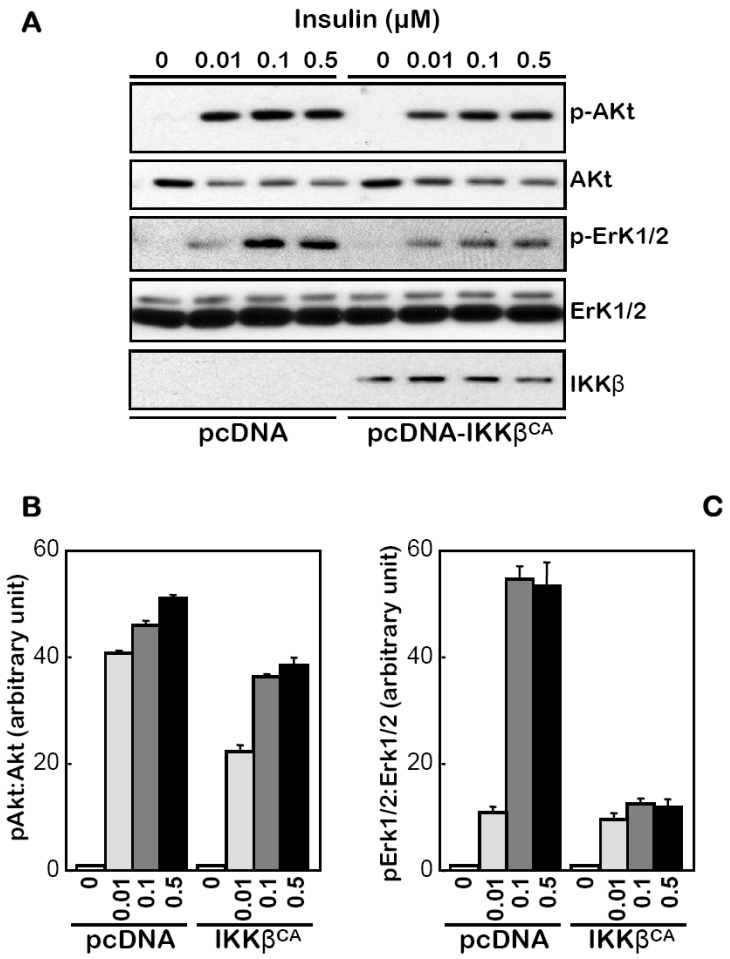

IKKβ/NF-κB activation in the GT1-7 cells reduces central insulin signaling. **A**. Hypothalamic GT1-7 cells were transfected with $IKK\beta^{CA}$-containing pcDNA 3.1 plasmid or the empty pcDNA 3.1, and stimulated with insulin at the indicated doses for 20 minutes. The cells were rapidly harvested, and the cell lysates were then prepared and analyzed for insulin signaling components

through Western blot analysis with the indicated antibodies. **B & C.** Phosphorylation levels of Akt (**B**) and Erk1/2 (**C**) were respectively quantitated and normalized according to their protein levels. Error bars reflect mean ± SEM.

Figure S11.

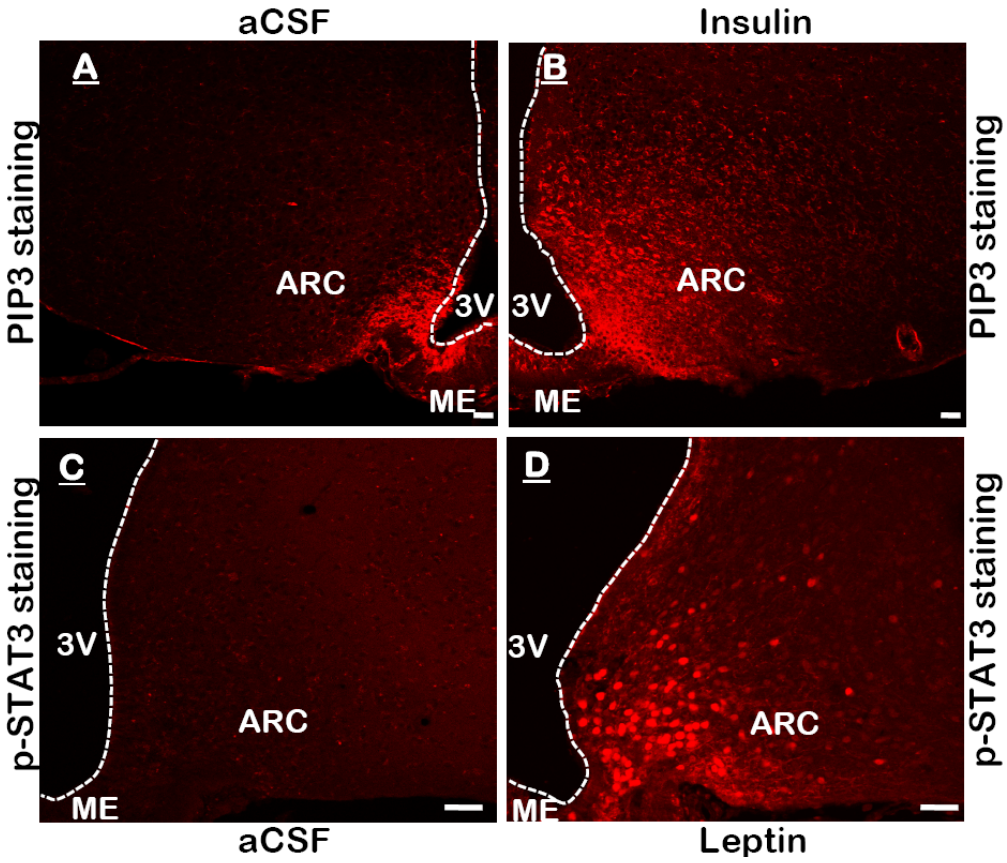

Immunostaining of insulin and leptin signaling in the MBH. Phosphorylation of phosphatidylinositol bisphosphate (PIP2) leading to the production of PIP3 (**A & B**) or the

phosphorylation of STAT3 (p-STAT3) (**C & D**) in response to an intra-third ventricle injection of insulin (**B**), leptin (**D**) or the empty vehicle aCSF (**A & C**). MBH sections were immunostained using the indicated antibodies. Broken lines outline 3V. 3V: third ventricle; ARC: arcuate nucleus. ME: median eminence. Bar = 100 μm.

Figure S12.

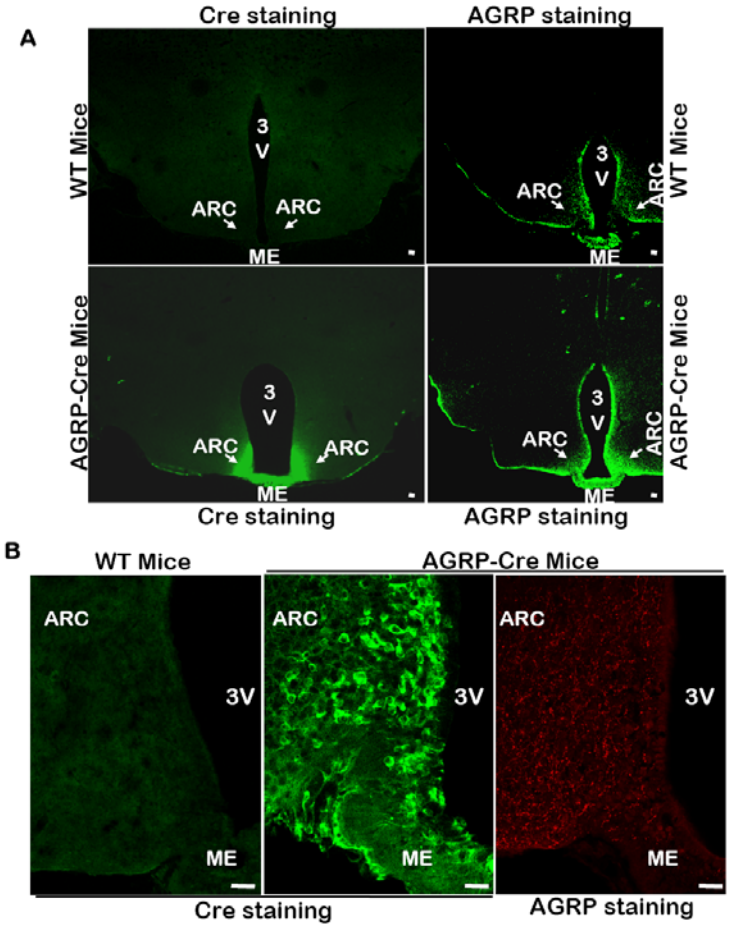

Hypothalamic immunostaining of Cre and AGRP for AGRP-Cre mice *vs.* WT mice. AGRP-Cre mice and the littermate WT mice were fixed and their brains across the hypothalamus were sectioned and immunostained using anti-Cre and anti-AGRP antibodies. Immunostaining is

presented both in low magnification (**A**) and in high magnification (**B**). 3V: third ventricle; ARC: arcuate nucleus. ME: median eminence. Bar = 50 μm.

Figure S13.

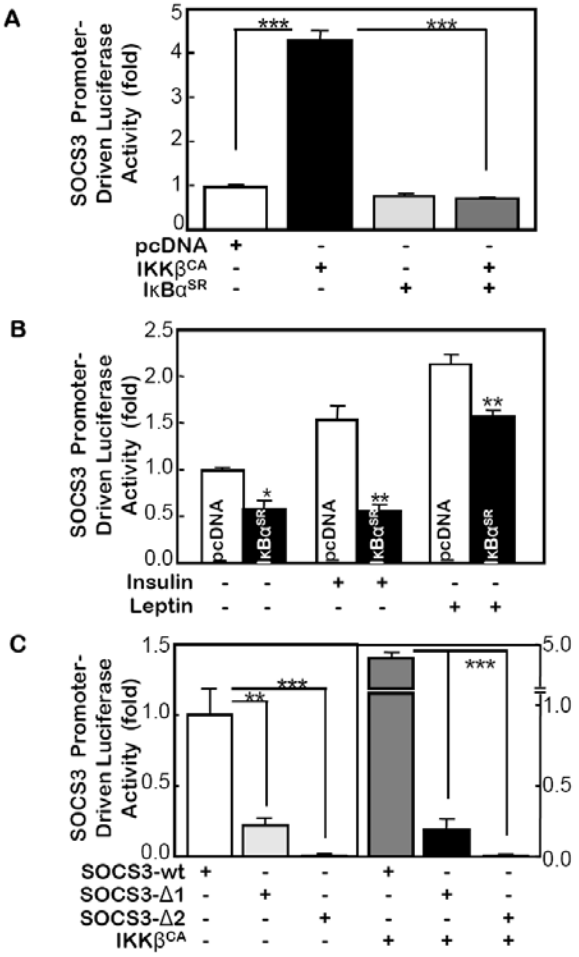

Regulation of mouse SOCS3 gene by IKKβ/NF-κB. **A.** A *firefly* luciferase pGL3 vector controlled by the wildtype SOCS3 promoter and a control plasmid, pRL-TK, that directs *renilla* luciferase, were co-transfected together with pcDNA-IKKβ^{CA}, pcDNA-IκBα^{SR}, or pcDNA into a

murine hypothalamic line, GT1-7 cells, or into a general murine cell line, C2C12 cells. **B.** The wildtype SOCS3 promoter-controlled pGL3 plasmid, pRL-TK, together with pcDNA-IκBα^{SR} or an empty pcDNA were transfected into HEK 293-lepR cells. Twenty-four hours post-transfection, the cells received a 6-hour treatment of insulin (10 nM) or leptin (1 ng/ml) or the empty buffer. **C.** A *firefly* pGL3 vector controlled by the wildtype SOCS3 promoter (SOCS3-wt) or a mutant SOCS3 promoter in which only the highlighted base pairs of NF-κB motif 1 (SOCS3-Δ1) or motif 2 (SOCS3-Δ2) were deleted, and the pRL-TK vector were co-transfected into GT1-7 cells or C2C12 cells, with or without co-transfection of pcDNA-IKKβ^{CA}. **A-C.** The *firefly* luciferase activity was normalized by *renilla* luciferase activity, and expressed as fold changes. (n = 3-4 per group; *$p<10^{-2}$, **$p<10^{-3}$, ***$p<10^{-4}$). Error bars reflect mean ± SEM.

Figure S14.

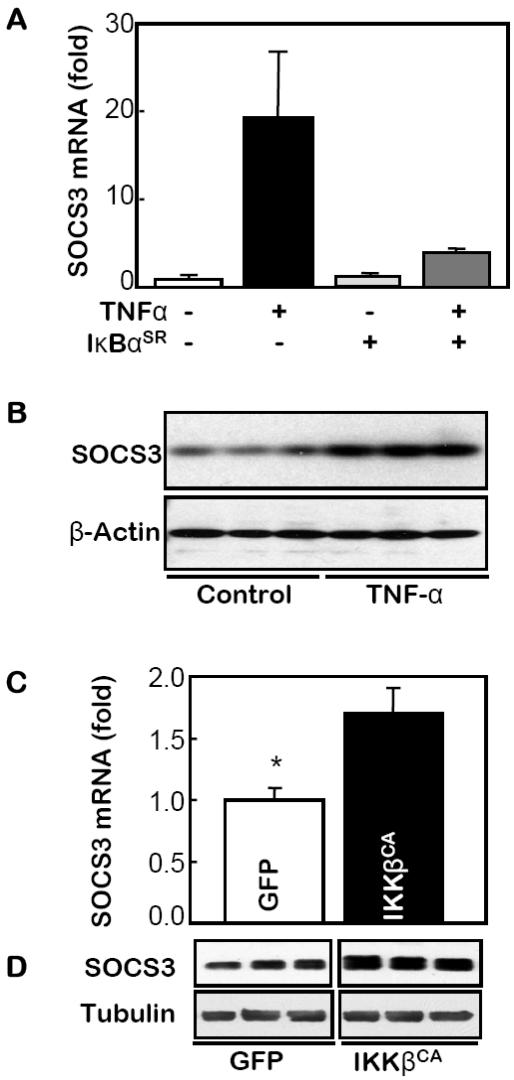

The effects of TNF-α and IKKβ/NF-κB on the expression of SOCS3. **A & B.** Relative mRNA levels (**A**) and the protein levels (**B**) of SOCS3 were measured in HEK 293 cells that, with the transfection of IκBα^{SR}-containing pcDNA 3.1 plasmid *vs*. the empty pcDNA 3.1 (**A**) or without transfection (**B**), were stimulated with TNF-α (+) (40 ng/ml) or the vehicle control (-) for 24 hours. The data represents three independent experiments. **C & D.** Relative mRNA levels (**C**)

and the protein levels (**D**) of SOCS3 were measured in the hypothalamus harvested from normal chow-fed C57BL/6 mice that received bilateral MBH injections of IKKβ^{CA}- and GFP-adenovirus. (n = 4-6 per group; *p<0.05).

Figure S15.

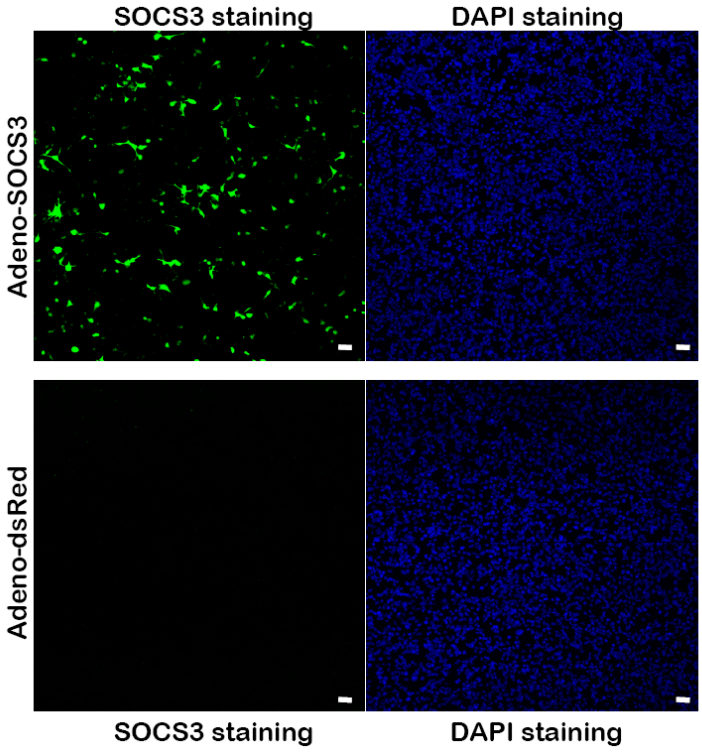

Immunostaining for virally-induced expression of SOCS3 in GT1-7 cells. GT1-7 cells were infected with an adenovirus containing SOCS3 (Adeno-SOCS3) or an irrelevant control DsRed (Adeno-DsRed). Following 36 hours post-viral infection, the cells were fixed and immunostained with the anti-SOCS3 antibody. The nuclear staining of DAPI revealed all the cells on the slide. Bar = 50 μm.

Figure S16.

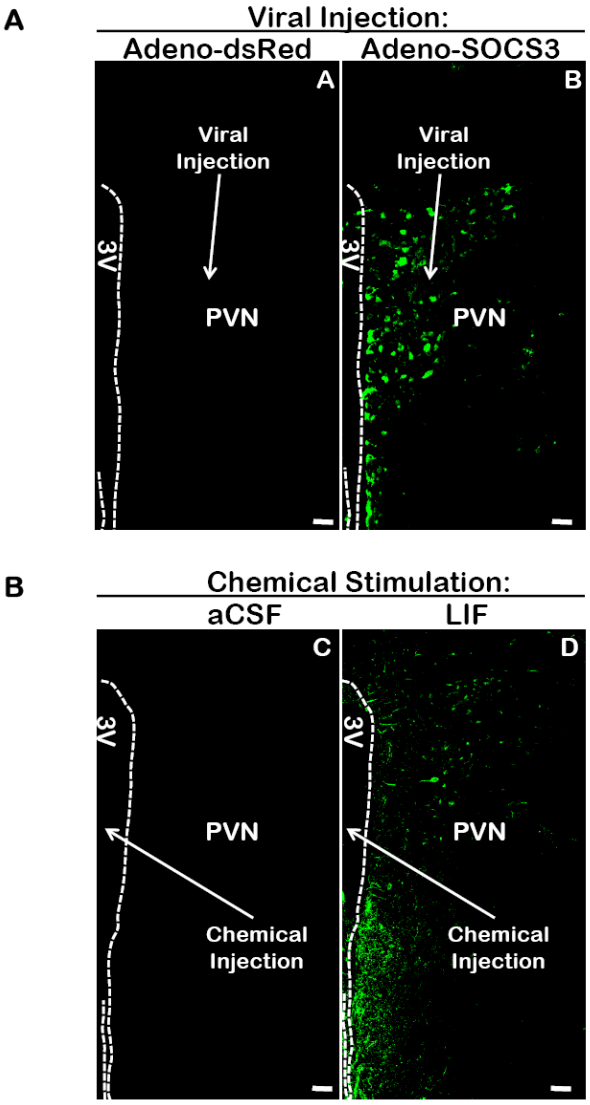

Immunostaining for viral- or hormonal-induced expression of SOCS3 in the PVN of the hypothalamus. Normal C57BL/6 mice received (**A**) intra-PVN injections of an adenovirus containing SOCS3 (Adeno-SOCS3) *vs.* an irrelevant control DsRed (Adeno-DsRed), or (**B**) intra-third ventricle infusions of 2 µg leukemia inhibitory factor (LIF) *vs.* the vehicle aCSF. One week post-viral injections or 2 hours post-LIF infusions, the mice were perfused, the brains were

fixed, and brain sections across the hypothalamus were stained with anti-SOCS3 antibody. PVN: paraventricular nucleus, 3V: third ventricle. Bar = 50 μm.